Int. J. Solids Structures, 1977, Vol. 13, pp 409–421 Pergamon Press. Printed in Great Britain

INFLATION OF SPHERICAL RUBBER BALLOONS

ALAN NEEDLEMAN
Division of Engineering, Brown University, Providence, RI 02912, U.S.A.

(*Received* 21 *June*; *revised* 17 *September* 1976)

Abstract—When a spherical rubber balloon of the sort used in meteorological applications is inflated, the onset of aspherical deformation is observed after the pressure maximum has been attained. Upon further inflation the balloon regains its spherical shape. Here, the rubber balloon is idealized as an elastic membrane and inflation is taken to be accomplished by a prescribed increase in enclosed volume. The axisymmetric equilibrium states of slightly imperfect membranes are determined numerically by means of the Ritz–Galerkin method. Several particular material models representative of the behavior of rubberlike solids are employed in order to illustrate a number of feautres associated with the aspherical deformation.

1. INTRODUCTION

When a rubber balloon of the type used to gather high altitude meteorological data is inflated the following course of events, depicted in [1, 2], is generally observed. There is a stiff initial stage during which the balloon is spherical. This persists until the pressure maximum is attained. After the pressure begins to fall with increasing inflation, the balloon becomes noticeably aspherical. As inflation continues, the asphericity eventually decreases and the balloon returns to a spherical shape.

The balloon can be idealized as a spherical membrane and the process of inflation is properly described as assigning the internal mass of fluid, not the pressure, so that no instability is necessarily encountered at the maximum pressure point. The rubberlike solids of which such balloons are made can be appropriately characterized as perfectly elastic materials, isotropic with respect to the ground state. Over the range of extensions of interest here these materials are also substantially incompressible.

Bifurcations of internally pressurized elastic spherical membranes into axisymmetric nonspherical modes have been studied in [3, 4] and [5] where, additionally, non-axisymmetric modes were considered. Of particular relevance here is the finding of Feodos'ev[3] that if a pressure minimum as well as a pressure maximum exists, a pair of bifurcation points for a given mode may occur between the maximum and minimum pressures. Feodos'ev[3] restricted attention to a particular form of strain energy function. Recently, an analysis along similar lines valid for a general form of strain energy function as well as for a class of inelastic solids yielded similar results[4]. In these studies the most critical mode is found to be one with modal deformations corresponding to local thinning at one pole.

In this paper a form of strain energy function proposed by Ogden[6] for incompressible isotropic elastic solids is employed and the bifurcation criteria given in [4] are specialized for particular material models representative of the behavior of rubberlike solids. Attention is then focussed on the behavior of imperfect pressurized spherical membranes made of such materials. The problem is formulated exactly within the context of membrane theory, but attention is restricted to axisymmetric deformations. The membrane is taken to be subject to a prescribed increase in enclosed volume. An initial imperfection is specified and the deformation history is calculated in an incremental manner by means of the Ritz–Galerkin method. At each stage of the loading history a modified Newton–Raphson procedure is employed to solve the resulting nonlinear equations. A comparison is made of the behavior of several material models.

2. PROBLEM FORMULATION

Three configurations of an axisymmetric closed membrane are considered; the reference configuration, which is taken to be that of a sphere of radius R_0 and uniform thickness t_0, the initial unstressed configuration and the current configuration. A Lagrangian formulation is employed and material points on the surface of the membrane are labelled by the coordinates θ and ϕ, where θ is the polar angle and ϕ is the longitudinal angle. Due to the assumed rotational

symmetry, all field quantities are independent of ϕ and the nonvanishing displacements are w, which is in the direction normal to the reference sphere and u which is tangential to the surface of the reference sphere in a meridian plane, see Fig. 1.

The unstressed configuration is specified by initial displacements u^I and w^I measured from the reference sphere and the initial, possibly nonuniform, thickness is denoted by t^I. The current configuration is also specified by displacements measured from the reference sphere, denoted by u^c and w^c, respectively, and the current thickness is t^c.

Principal axis notation is employed and the following conventions are adopted; subscripts range from 1 to 2, with subscript 1 denoting principal values associated with the θ-direction and the subscript 2 denoting corresponding values in the ϕ-direction, while $(\,)_{,\theta}$ denotes differentiation with respect to θ.

The current configuration of the membrane is specified by the following three quantities,

$$e_1^c = \frac{1}{R_0}(w^c + u^c_{,\theta})$$

$$e_2^c = \frac{1}{R_0}(w^c + \cot\theta\, u^c) \tag{1}$$

$$\psi^c = \frac{1}{R_0}(w^c_{,\theta} - u^c).$$

Here, e_1^c and e_2^c are the principal values of the linear strain tensor and ψ^c is a measure of the rotation of the normal to the membrane, in that the projection of the normal to the membrane in its current configuration on the tangent to the reference sphere is proportional to ψ^c.

The principal stretches, λ_i^c, and the principal values of the Lagrangian strain tensor, η_i^c, are given in terms of e_1^c, e_2^c and ψ^c by,

$$\lambda_1^c = [(1+e_1^c)^2 + (\psi^c)^2]^{1/2} \qquad \lambda_2^c = 1 + e_2^c \tag{2}$$

$$\eta_1^c = e_1^c + \frac{1}{2}(e_1^c)^2 + \frac{1}{2}(\psi^c)^2 \qquad \eta_2^c = e_2^c + \frac{1}{2}(e_2^c)^2. \tag{3}$$

The quantities, e_i^I, ψ^I, λ_i^I and η_i^I are given by expressions of the form (1)–(3) with w^c and u^c replaced by w^I and u^I.

The difference between the volume enclosed by the membrane in its current configuration and

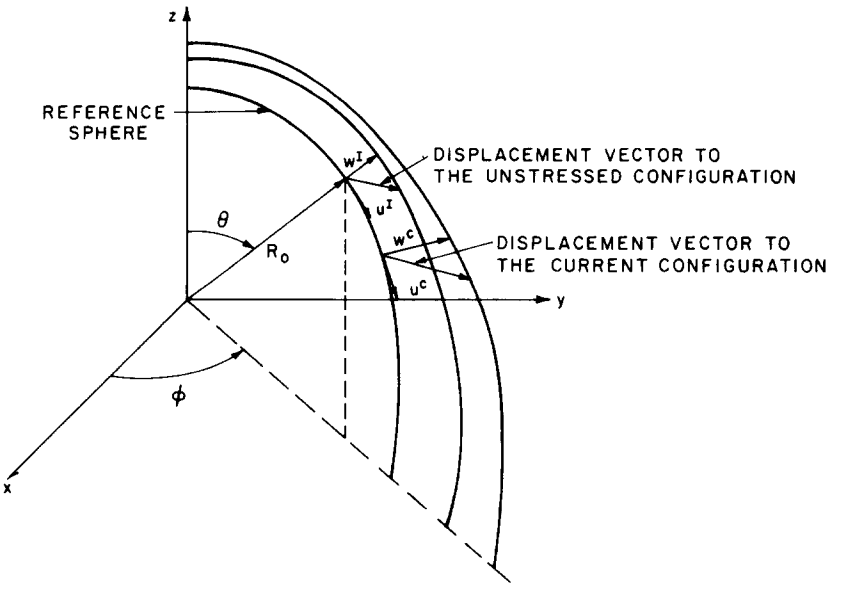

Fig. 1. Coordinate system and displacement vectors to the unstressed and current configurations.

that enclosed by the reference sphere is denoted by ΔV^c and is given by,

$$\Delta V^c = 2\pi R_0^2 \int_0^\pi \left[w^c + \frac{1}{2} w^c (e_1{}^c + e_2{}^c) + \frac{1}{3} w^c e_1{}^c e_2{}^c - \frac{1}{2} u^c \psi^c - \frac{1}{3} u^c \psi^c e_2{}^c \right] \sin\theta \, d\theta. \tag{4}$$

Analogously, the difference between the volume enclosed by the membrane in its initial configuration and that enclosed by the reference sphere, denoted by ΔV^I, is given by an expression of the form (4) with superscripts "c" replaced by superscripts "I".

Thus, the change in enclosed volume from the initial state to the current state, ΔV, is

$$\Delta V = \Delta V^c - \Delta V^I. \tag{5}$$

Here, and subsequently, quantities associated with the deformation from the initial state to the current state have no superscript.

The principal stretches from the initial configuration to the current configuration are

$$\lambda_i = \lambda_i{}^c / \lambda_i{}^I \qquad \text{(no sum)}. \tag{6}$$

The materials considered here are taken to be incompressible and the incompressibility condition is expressed by the relation,

$$\lambda_1{}^c \lambda_2{}^c \left[\frac{t^c}{t_0} \right] = \lambda_1{}^I \lambda_2{}^I \left[\frac{t^I}{t_0} \right]. \tag{7}$$

Inflation is taken to be accomplished by some device that supplies given quantities of fluid to the volume enclosed by the membrane. If the membrane is attached to a large reservoir that can supply the needed quantities of fluid at constant pressure, it is appropriate to consider the pressure to be the prescribed quantity. More often inflation is achieved by some device for which the flow rate depends on the pressure. The most realistic alternative is to consider the mass of fluid required for inflation to be the prescribed quantity and to account for the pressure dependence of the fluid density. However, if the fluid is incompressible or nearly so, the volume of fluid rather than the mass may be taken to be prescribed. This corresponds to the limiting case of an infinitely stiff loading device and this idealization will be employed here.

The principle of virtual work takes the form

$$2\pi R_0^2 t_0 \int_0^\pi \lambda_1{}^I \lambda_2{}^I \left[\frac{t^I}{t_0} \right] \left[\sigma_1 \frac{\delta \eta_1{}^c}{(\lambda_1{}^c)^2} + \sigma_2 \frac{\delta \eta_2{}^c}{(\lambda_2{}^c)^2} \right] \sin\theta \, d\theta = p\delta(\Delta V) = p\delta(\Delta V^c) \tag{8}$$

where p is the pressure and

$$\delta \eta_1{}^c = (1 + e_1{}^c)\delta e_1{}^c + \psi^c \delta \psi^c \qquad \delta \eta_2{}^c = (1 + e_2{}^c)\delta e_2{}^c \tag{9}$$

while $\delta e_1{}^c$, $\delta e_2{}^c$ and $\delta \psi^c$ are related to the displacement variations δw^c and δu^c by (1). The principal stresses, σ_i, appearing in (8) are regarded as being thickness average quantities.

The relation (6) enables equivalent alternative expressions to be employed for the internal virtual work. The one given in (8) is the most convenient for the present purposes.

Integrating by parts and employing the essential boundary condition that u vanish at $\theta = 0$ and π, the expression for $\delta(\Delta V^c)$ can be written in the form

$$\delta(\Delta V^c) = 2\pi R_0^2 \int_0^\pi [\delta w^c (1 + e_1{}^c + e_2{}^c + e_1{}^c e_2{}^c) - \delta u^c (1 + e_2{}^c)\psi^c] \sin\theta \, d\theta. \tag{10}$$

The expressions employed in the principle of virtual work (8) and (10) may be obtained by specializing the general nonlinear membrane formulas in [7].

For the isotropic incompressible elastic solids considered here, the existence of a strain energy function is postulated. This strain energy function is an isotropic function of the principal

stretches λ_1, λ_2 and λ_3, where λ_3 is given by $1/(\lambda_1\lambda_2)$. The usual practice in elasticity theory is to express the strain energy function in terms of two independent strain invariants rather than directly in terms of the principal stretches. This often complicates calculations, particularly of the instantaneous moduli. An attractive alternative, suggested by Hill [9], is to write the strain energy function directly in terms of the principal stretches. Here, the strain energy function is written in the form proposed by Ogden [6].

$$\Phi(\lambda_1, \lambda_2, \lambda_3) = \sum_r \frac{\mu_r}{\alpha_r}[\lambda_1^{\alpha_r} + \lambda_1^{\alpha_r} + \lambda_3^{\alpha_r} - 3] \tag{11}$$†

where μ_r and α_r are constants and the summation on r extends over as many terms as are necessary to characterize a particular material. In (11), α_r may take on any nonzero real value.

The principal values of the Cauchy, or true stress tensor are given by,

$$\sigma_i = \lambda_i \frac{\partial \Phi}{\partial \lambda_i} + \sigma_m \qquad (i = 1, 2, 3, \text{ no sum}) \tag{12}$$

where σ_m is the mean normal stress, which within the context of membrane theory is determined by the requirement that $\sigma_3 = 0$. Thus, from (11) and (12)

$$\begin{aligned} \sigma_1 &= \sum \mu_r[\lambda_1^{\alpha_r} - (\lambda_1\lambda_2)^{-\alpha_r}] \\ \sigma_2 &= \sum \mu_r[\lambda_2^{\alpha_r} - (\lambda_1\lambda_2)^{-\alpha_r}]. \end{aligned} \tag{13}$$

The plane stress instantaneous moduli $\mathbf{L}$ relate increments of Cauchy stress $\dot{\sigma}_i$ and logarithmic strain $\dot{\epsilon}_i$,

$$\dot{\sigma}_i = L_{ij}\dot{\epsilon}_j$$

where

$$\dot{\epsilon}_j = \dot{\lambda}_j/\lambda_j \qquad \text{(no sum)}. \tag{14a}$$

From (11) $\mathbf{L}$ is readily found to be given by

$$\begin{aligned} L_{11} &= \sum_r \mu_r\alpha_r[\lambda_1^{\alpha_r} + (\lambda_1\lambda_2)^{-\alpha_r}] \\ L_{22} &= \sum_r \mu_r\alpha_r[\lambda_2^{\alpha_r} + (\lambda_1\lambda_2)^{-\alpha_r}] \\ L_{12} &= L_{21} = \sum_r \mu_r\alpha_r(\lambda_1\lambda_2)^{-\alpha_r}. \end{aligned} \tag{14b}$$

It will be assumed that for any given material the appropriate values of μ_r and α_r are such that the moduli $\mathbf{L}$ are positive definite in the ground state.

For a perfect sphere, $\lambda_1^I = \lambda_2^I = 1$, $t^I = t_0$, one solution to the present problem, available for all values of prescribed change in enclosed volume, corresponds to the spherically symmetric state

$$\begin{aligned} &\lambda_1 = \lambda_2 = \lambda_0 = 1 + \frac{w_0}{R_0} \qquad \sigma_1 = \sigma_2 = \sigma_0 \\ &p_0 = 2\left(\frac{t_0}{R_0}\right)\frac{\sigma_0}{\lambda_0^3}. \end{aligned} \tag{15}$$

From (15) and (14) it can be shown that a maximum or minimum pressure is attained when σ_0 achieves the value

$$\sigma_m = \frac{1}{3}\sum \mu_r\alpha_r[\lambda_m^{\alpha_r} + 2\lambda_m^{-2\alpha_r}] \tag{16}$$

where λ_m is the value of λ_0 at the maximum or minimum pressure.

Bifurcation of an internally pressurized spherical membrane into axisymmetric nonspherical

†The one term version of (11) is due to Prof. R. Hill, see [6] footnote on p. 567.

modes is also possible[3–5]. A complete set of axisymmetric eigenmodes is given by modal displacements w^* and u^* of the form[3–5]

$$w^* = w_n^* P_n(\cos\theta) \qquad u^* = u_n^* \frac{dP_n(\cos\theta)}{d\theta} \tag{17}$$

where P_n is the Legendre polynomial of degree $n(=1,2,3\ldots)$.

The mode giving the smallest bifurcation stretch, λ_c, is the one with $n = 1$. The criterion for bifurcation into this mode is [4]

$$\sigma_c = \frac{1}{2}\sum_r \mu_r\alpha_r[\lambda_c^{\alpha_r} + 2\lambda_c^{-2\alpha_r}]. \tag{18}$$

In this mode it is necessary to constrain the membrane against rigid body translation. This may be accomplished by arbitrarily setting $w_1 = 0$. The bifurcation mode deflections correspond to thinning at one pole with a corresponding thickening at the other.

Denoting the instantaneous biaxial stiffness by L_0, where

$$L_0 = L_{11} + L_{12} = \sum_r \mu_r\alpha_r[\lambda_0^{\alpha_r} + 2\lambda_0^{-2\alpha_r}] \tag{19a}$$

eqns (16) and (18) take the concise forms

$$(\sigma_0/L_0)_m = \frac{1}{3} \tag{19b}$$

$$(\sigma_0/L_0)_c = \frac{1}{2}. \tag{19c}$$

From eqns (19b) and (19c) it is evident that a curve of σ_0/L_0 vs λ_0 reveals the nature of the bifurcation behavior of a spherical membrane. Essentially this plot was considered by Feodos'ev[3] who, however, employed L_0/σ_0 as the dependent variable. Initially, σ_0/L_0, is zero. As deformation proceeds, this quantity increases and if it attains the value 1/3 a pressure maximum takes place. A bifurcation into the $n = 1$ mode occurs if σ_0/L_0 reaches 1/2. A further increase in σ_0/L_0 is needed for bifurcation into a higher order mode, the precise amount depending on $L_{11} - L_{12}$ as well as L_0[3, 4]. For many rubberlike solids σ_0/L_0 reaches a maximum and then decreases. If this maximum exceeds 1/2, a second bifurcation point for the $n = 1$ mode is encountered. Finally, if σ_0/L_0 falls to 1/3 a pressure minimum is attained. For meteorological balloons both a pressure maximum and minimum may occur, so that if σ_0/L_0 exceeds 1/2 there will be two bifurcation points for the $n = 1$ mode.

In this study attention will be focussed primarily on two specific examples of the stress-strain law (11). The first, subsequently referred to as *Material I* and characterized by the parameters,

$$\begin{aligned} &\alpha_1 = 1.3 \qquad \alpha_2 = 5.0 \qquad \alpha_3 = -2.0 \\ &\mu_1 = 6.3 \qquad \mu_2 = 0.012 \qquad \mu_3 = -0.1 \end{aligned} \tag{20}$$

was found by Ogden[6] to give excellent agreement, for a variety of homogeneous stress states with some experimental data of Treloar[8] for a particular rubber. The curve of stress, nondimensionalized with respect to $\Sigma\,\mu_r\alpha_r$, which is twice the ground state shear modulus, vs stretch for this material in equal biaxial tension is shown in Fig. 2.

Figure 3 depicts plots of the nondimensional pressure, p^*, and the stress modulus ratio, σ_0/L_0, vs stretch λ_0. The nondimensional pressure, p^*, is defined by

$$p^* = \frac{p_0}{2\left(\frac{t_0}{R_0}\right)\sum_r \mu_r\alpha_r}. \tag{21}$$

The maximum and minimum pressures are attained at $\lambda_0 = 1.38$ and $\lambda_0 = 4.32$, respectively, and these correspond to the two values of λ_0 for which (19b) is satisfied. The bifurcation criterion

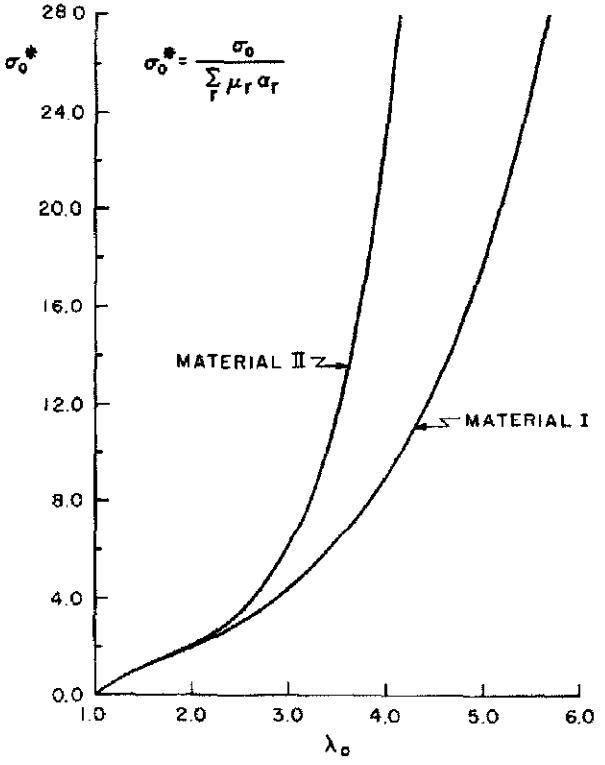

Fig. 2. Curves of stress vs stretch for Material I and Material II in equal biaxial tension. The material parameters are given by eqns (20) and (22) of the text, respectively.

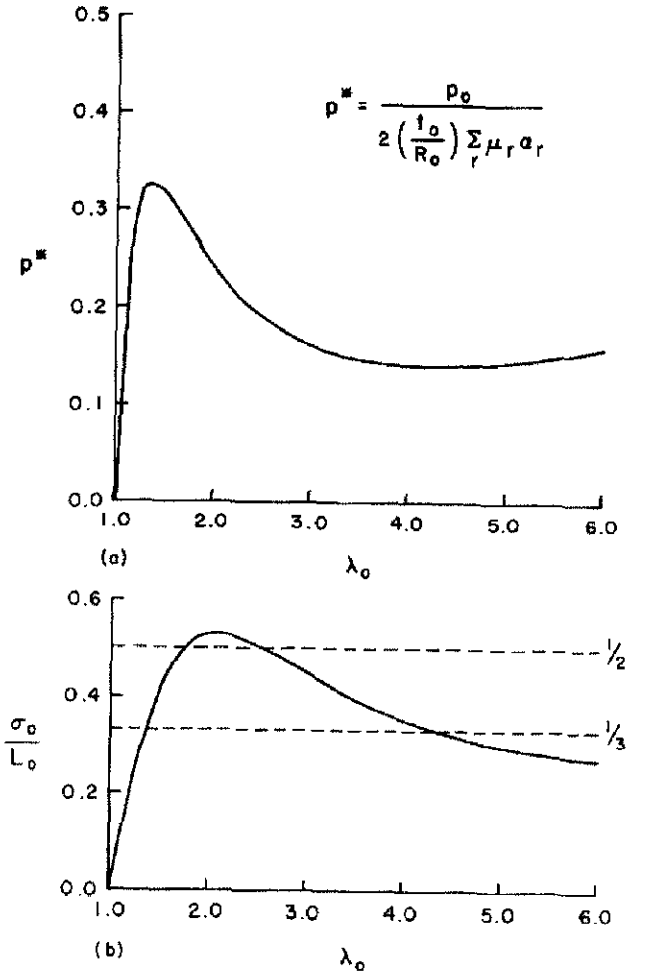

Fig. 3. Response of Material I in the spherically symmetric state. (a) curve of pressure vs stretch and (b) curve of stress divided by instantaneous biaxial stiffness vs stretch. The material parameters are given by eqn (20) of the text.

(19c) is also met for two values of λ_0, namely 1.77 and 2.54. Between these two values, σ_0/L_0 achieves a maximum, $\sigma_0/L_0 = 0.528$, which occurs when $\lambda_0 = 2.10$. The possibility of bifurcation into a higher, $n > 1$, mode was also investigated and it was found that no such bifurcations occur for this material.

For comparison purposes *Material II*, characterized by the parameters

$$\begin{aligned} \alpha_1 &= 0.8 \quad & \alpha_2 &= 6.0 \quad & \alpha_3 &= 0.5 \\ \mu_1 &= 3.0 \quad & \mu_2 &= 0.016 \quad & \mu_3 &= 2.0 \end{aligned} \tag{22}$$

is considered. The equal biaxial tension stress-stretch curve for this material is also shown in Fig. 2.

Plots of nondimensionalized pressure, p^*, and the stress to modulus ratio, σ_0/L_0, for this set of parameters are depicted in Fig. 4. The maximum and minimum pressures occur at $\lambda_0 = 1.38$ and $\lambda_0 = 2.66$, respectively. The two values of λ_0 for which the bifurcation criterion for the $n = 1$ mode is satisfied are $\lambda_0 = 1.78$ and $\lambda_0 = 1.96$. Bifurcations into higher order ($n > 1$) modes are not possible for this material.

For Material II there is a much sharper maximum pressure peak and the pressure increases much more rapidly after the minimum value has been attained than for Material I. Also, note that the excursion of the ratio σ_0/L_0 above 1/2 is somewhat less than in the previous example. Here, the maximum value, $\sigma_0/L_0 = 0.505$, is attained at $\lambda_0 = 1.86$.

The difference between these two material models of principal relevance here is the amount

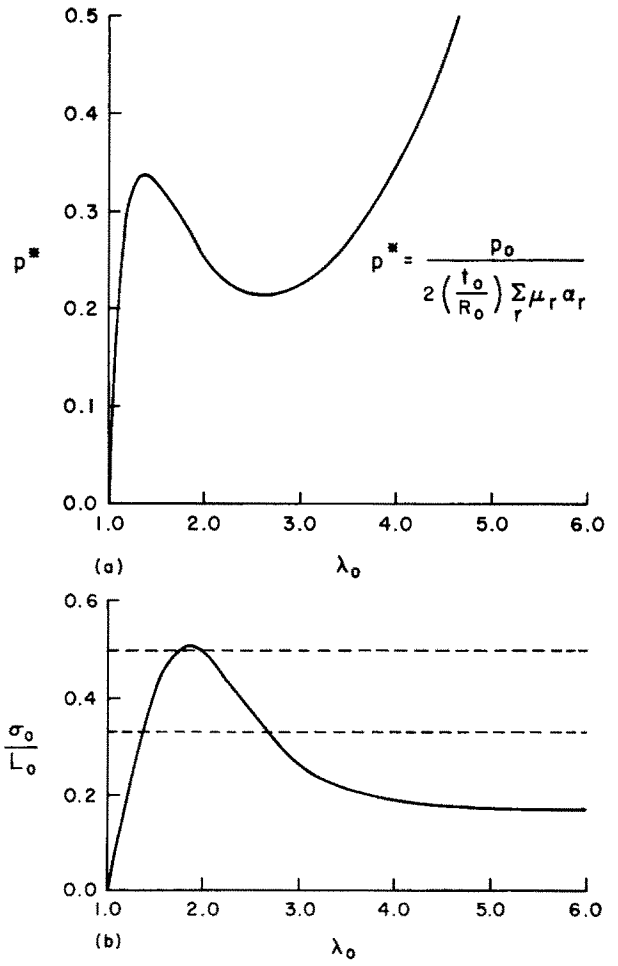

Fig. 4. Response of Material II in the spherically symmetric state, (a) curve of pressure vs stretch and (b) curve of stress divided by instantaneous biaxial stiffness vs stretch. The material parameters are given by eqn (22) of the text.

of the excursion of σ_0/L_0 above 1/2. It is of interest to determine whether or not the amount of this excursion correlated with the amount of asphericity that develops.

Neither of the material models considered here represents the behavior of the specific rubber, DuPont Neoprene (polychloroprene), employed in Alexander's experimental study[1], although the behavior of Material I appears qualitatively similar. Alexander[1] employed his representation of the strain energy function in Feodos'ev's analysis[3] and found bifurcation points, for the $n = 1$ mode, at $\lambda_0 = 1.6$ and $\lambda_0 = 4.3$. In [1] the same strain energy function is found to predict a pressure minimum at $\lambda_0 = 3.8$. The occurrence of the minimum pressure between the two bifurcation points is inconsistent with the analysis given in [3] as well as with the one given here.

3. NUMERICAL METHOD

The initial shape and thickness of the membrane are specified by w^I, u^I and t^I. Here, attention is confined to membranes that are nearly spherical. This enables a Ritz–Galerkin method to be employed where the displacements w^c and u^c are expanded in terms of Legendre polynomials of the form (17) so that,

$$w^c = \sum_{n=1}^{N} w_n{}^c P_n(\cos\theta) \qquad u^c = \sum_{n=1}^{N} u_n{}^c \frac{dP_n(\cos\theta)}{d\theta}. \tag{23}$$

The rigid body translation mode is supressed by taking $w_1{}^c \equiv 0$. The quantities $e_1{}^c$, $e_2{}^c$ and ψ^c in (1) are given by,

$$\begin{aligned} e_1{}^c &= \frac{1}{R_0}\sum_n [w_n{}^c P_n + u_n{}^c (DP_n \cos\theta - n(n+1)P_n)] \\ e_1{}^c &= \frac{1}{R_0}\sum_n [w_n{}^c P_n + u_n{}^c DP_n \cos\theta] \\ \psi^c &= \frac{1}{R_0}\sum_n [u_n{}^c - w_n{}^c] DP_n \sin\theta \end{aligned} \tag{24}$$

where

$$DP_n \equiv \frac{dP_n(\cos\theta)}{d(\cos\theta)}. \tag{25}$$

The principal stretches, $\lambda_i{}^c$, and the principal strains, $\eta_i{}^c$, can then be calculated from (24) by (2) and (3).

Expanding the principal of virtual work (8) about some given state gives to lowest order,

$$\begin{aligned} &2\pi R_0{}^2 t_0 \int_0^{\pi} \lambda_1{}^I \lambda_2{}^I \left(\frac{t^I}{t_0}\right)\left[\left(\frac{\dot\sigma_1}{(\lambda_1{}^c)^2} - \frac{2\sigma_1}{(\lambda_1{}^c)^4}\dot\eta_1\right)\delta\eta_1{}^c + \left(\frac{\dot\sigma_2}{(\lambda_2{}^c)^2} - \frac{\sigma_2}{(\lambda_2{}^c)^4}\dot\eta_2\right)\delta\eta_2{}^c \right. \\ &\qquad \left. + \frac{\sigma_1}{(\lambda_1{}^c)^2}(\dot e_1{}^c \delta e_1{}^c + \dot\psi^c \delta\psi^c)\right] \sin\theta\, d\theta \\ &\quad = 2\pi R_0{}^2 \dot p \int_0^{\pi} [(1 + e_1{}^c + e_2{}^c + e_1{}^c e_2{}^c)\delta w^c - \psi^c (1 + e_2{}^c)\delta u^c] \sin\theta\, d\theta \\ &\qquad + 2\pi R_0{}^2 p \int_0^{\pi} [\dot e_1{}^c + \dot e_2{}^c + e_1{}^c \dot e_2{}^c + \dot e_1{}^c e_2{}^c)\delta w^c - \{\dot\psi^c (1 + e_2{}^c) + \psi^c \dot e_2{}^c\}\delta u^c] \sin\theta\, d\theta \\ &\qquad - \left\{2\pi R_0{}^2 t_0 \int_0^{\pi} \lambda_1{}^I \lambda_2{}^I \left(\frac{t^I}{t_0}\right)\left[\sigma_1 \frac{\delta\eta_1{}^c}{(\lambda_1{}^c)^2} + \sigma_2 \frac{\delta\eta_2{}^c}{(\lambda_2{}^c)^2}\right] \sin\theta\, d\theta - p\delta(\Delta V^c)\right\}. \end{aligned} \tag{26}$$

Here, $(\dot{})$ denotes the change in quantities from the given state while $e_1{}^c$, ψ^c, σ_i, p, ΔV^c and $\delta\eta_i{}^c$ are evaluated at the given state.

Employing the moduli (14b), the expansions (23) and (24) and integrating with respect to θ transforms (26) into a coupled set of linear algebraic equations for the $2N + 1$ quantities $\dot w_n{}^c$, $\dot u_n{}^c$ and $\dot p$. The numerical integration was carried out by dividing the interval $[0, \pi]$ into segments and employing four point Gaussian integration within each segment.

The resulting equations were solved by a combined incremental iterative procedure that proceeded as follows. At a given stage of the loading history values of the $2N+1$ parameters, u_n^c, w_n^c and p satisfying (8) are assumed known. An increment of one of these parameters is taken to be prescribed. The incremental eqn (26) is solved for the remaining $2N$ parameters with the term in braces set equal to zero since the given state satisfies equilibrium. The prescribed parameter is then regarded as fixed and (26) is solved repeatedly, updating u_n^c, w_n^c and p after each solution. The iterations are continued until the maximum change in $\dot{u}_n^c/R_0$, $\dot{w}_n^c/R_0$ and the nondimensional pressure increment, $\dot{p}^*$, is less than some predetermined tolerance which for the calculations reported on here is taken to be 10^{-4}. Over most of the loading history five or six iterations were sufficient to obtain the desired accuracy. However, over a certain part of the loading history it was found that the Newton–Raphson procedure diverged. The nature of the divergence was a growing oscillation of the incremental amplitudes and this enabled a simple corrective method to be employed. If such an oscillation was detected, linear interpolation between the most recently computed iterates of opposite sign, rather than the Newton–Raphson values, was employed to obtain the next correction. This procedure was continued until the amplitude of the oscillations was sufficiently small and then the Newton–Raphson method was employed again. It was found necessary to switch back to the Newton–Raphson procedure, when the oscillations became less severe, since the asymptotic convergence rate of the linear interpolation prodecure was unsatisfactory. Of course, the criterion for switching to the Newton–Raphson iterate was somewhat arbitrary and on occasion this procedure would begin to diverge again. In such a case, interpolation was re-employed. When this rather involved iteration method needed to be employed, up to 30 iterations were required for convergence, even though small increments were used. This poor convergence occurred during a clearly identifiable part of the loading history, which will be pointed out when the numerical results are presented.

The parameter to be prescribed in a given increment was chosen by a procedure employed by Dr. V. Tvergaard of the Technical University of Denmark (private communication, 1973). The parameter that had the numerically largest incremental value in the previous increment is prescribed at the next step. This enables numerical instabilities associated with local maxima or minima in one or more of the quantities u_n, w_n and p to be avoided.

The present computations were carried out with $N = 3$ and the interval $[0, \pi]$ was divided into five segments so that twenty integration points were employed. Throughout the deformation histories computed here u_3^c and w_3^c remained small compared to w_0^c and u_1^c. A portion of one computation was repeated including w_4^c and u_4^c. Even though this was near the point of maximum asphericity including these terms had no appreciable effect. Furthermore, some computations were repeated with forty integration points and these results also were nearly identical to those obtained with twenty integration points.

4. NUMERICAL RESULTS FOR IMPERFECT SPHERICAL MEMBRANES

The results of the numerical calculations for imperfect spherical membranes with Material I are depicted in Fig. 5, and the corresponding results for Material II are shown in Fig. 6. In these figures the amplitude, ξ_1, of the bifurcation mode is defined by

$$\xi_1 = \frac{|u_1^c|}{R_0}. \tag{27}$$

The absolute value is employed in (27) since there is symmetry about $\xi_1 = 0$. In Figs. 5 and 6 ξ_1 is plotted against $\hat{\lambda}_0$ which is the ratio of the mean radius of the deformed membrane to the radius of the reference sphere. Thus,

$$\hat{\lambda}_0 = 1 + \frac{w_0^c}{R_0}. \tag{28}$$

When the asphericity vanishes $\hat{\lambda}_0 = \lambda_0$.

An initial imperfection can be specified in several ways. In one case an initial stress free displacement in the shape of the bifurcation mode is prescribed. Without loss in generality w_1^I is taken to be zero and analogous to (27) $\bar{\xi}_1$ is defined as $|u_1^I|/R_0$. The initial thickness distribution is then determined by requiring that the deformation from the reference sphere to the unstressed

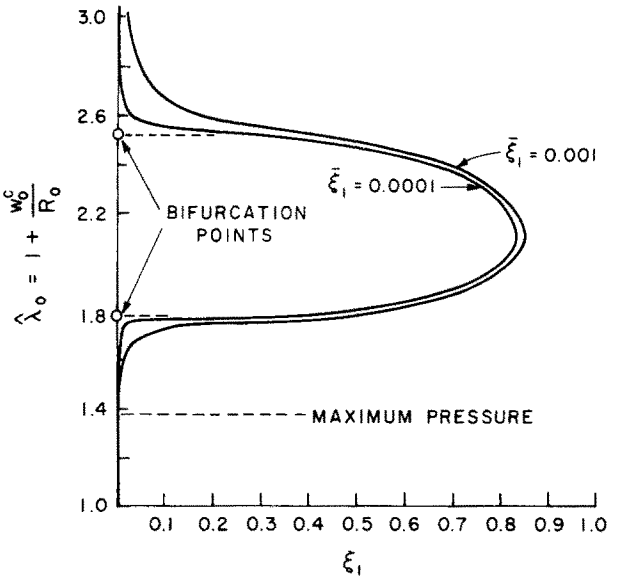

Fig. 5. Curves of bifurcation mode amplitude vs mean radius for Material I with two different initial imperfection amplitudes. The material parameters are given by eqn (20) of the text.

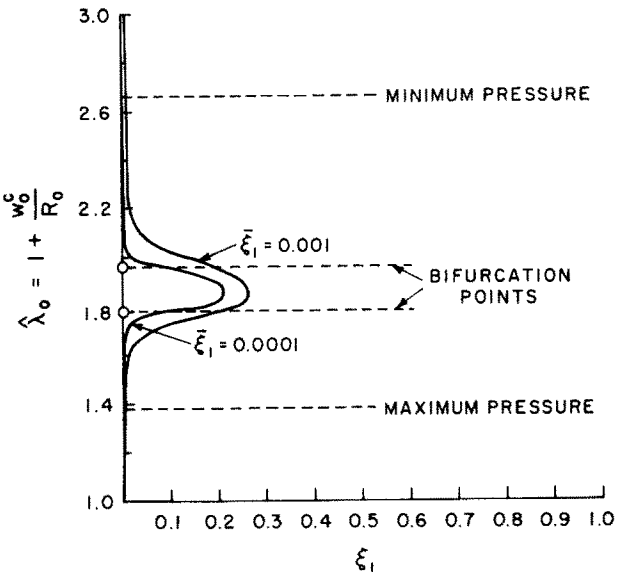

Fig. 6. Curves of bifurcation mode amplitude vs mean radius for Material II with two different initial imperfection amplitudes. The material parameters are given by eqn (22) of the text.

state satisfy incompressibility. Another type of initial imperfection employs the initial thickness distribution calculated in the above manner but takes the initial deviation from sphericity to be zero. In this case the deformation from the reference sphere to the unstressed state does not satisfy incompressibility.

For both types of initial imperfection the maximum deviation of the absolute value of t'/t_0 from unity is approximately $2\bar{\xi}_1$ for sufficiently small $\bar{\xi}_1$. For the results displayed in Figs. 5 and 6 the second type of imperfection was employed. Some calculations were repeated using the first type of imperfection without appreciably altering the results. On the other hand, if in the unstressed state the thickness is uniform but there is a small initial deviation from sphericity, a perturbation analysis [4] and numerical calculations carried out here reveal that in the limit $\lambda_0 \to \lambda_c$ the slightly aspherical membrane essentially bifurcates as a perfect sphere. Thus, the important aspect of any initial imperfection is the deviation from uniform thickness and small initial deviations from sphericity do not play a significant role.

In the calculations displayed in Figs. 5 and 6 two imperfection amplitudes were employed $\bar{\xi}_1 = 0.001$ and $\bar{\xi}_1 = 0.0001$. All curves obtained here are qualitatively similar in that very little growth of ξ_1 is evident until the vicinity of the first bifurcation point, the asphericity then grows rapidly, reaches a maximum and then decreases. In the vicinity of the second bifurcation point the asphericity essentially disappears. Note that nothing special occurs at the maximum pressure point.

For the prescribed change in enclosed volume loading considered here, stability, in the usual engineering sense, depends on whether or not the current volume, V^c, is monotonically increasing along the equilibrium path. Here,

$$V^c = \Delta V^c + V_0 \tag{29}$$

where V_0 is the volume enclosed by the reference sphere and ΔV^c is given by (4). A more convenient measure of the current volume enclosed by the membrane is provided by

$$\hat{\lambda} \equiv (V^c/V_0)^{1/3}. \tag{33}$$

For spherically symmetric deformation $\hat{\lambda} = \hat{\lambda}_0 = \lambda_0$. When there is aspherical deformation monotonically increasing $\hat{\lambda}_0$ along the equilibrium path does not guarantee monotonically increasing $\hat{\lambda}$ and vice versa. However, for all the equilibrium paths displayed in Figs. 5 and 6 $\hat{\lambda}$ as well as $\hat{\lambda}_0$ is increasing monotonically so that for the loading condition employed here the deformation is stable along these paths.

There are several other features common to the results presented in Figs. 5 and 6. One is that the amplitudes of the higher order terms u_2/R_0, w_2/R_0, etc., remain small compared to ξ_1. For example with Material I and $\bar{\xi}_1 = 0.001$, the maximum value of ξ_1 achieved is 0.85, while the next largest mode amplitude, w_2/R_0, attains a maximum of 0.12. Thus, although these higher order modes may play a significant role in equilibrating the membrane in the aspherical state their influence on the deformed shape is slight. Another common feature is that the pressure is monotonically decreasing along the aspherical equilibrium path.

As stated in Section 3, the part of the loading history which caused the greatest numerical difficulty can be identified on the curves in Figs. 5 and 6. It is the region in the vicinity of the point of maximum asphericity. Convergence difficulties usually were greatest near where the rates of change of $\hat{\lambda}_0$ and ξ_1 are about the same. Convergence of the numerical method was often somewhat better at the actual maximum of asphericity.

For Material I, there is very little difference in the maximum value of ξ_1 attained for the two imperfection values considered, with the smaller imperfection amplitude $(\xi_1)_{max} = 0.83$ while with the larger imperfection amplitude, $(\xi_1)_{max} = 0.85$. In both cases this maximum is attained at $\hat{\lambda}_0 = 2.12$, which is very close to the value at which (σ_0/L_0) attained its maximum in Fig. 3. Although the plot of ξ_1 vs $\hat{\lambda}_0$ provides the most graphic picture of the asphericity, a more appropriate indication of the degree of asphericity is provided by the quantity $u_1^c/\hat{\lambda}_0 R_0$, which is the ratio of the amplitude of the aspherical mode to the current mean radius and is approximately 0.4 at maximum asphericity in Fig. 5. Another measure of asphericity is $\hat{\lambda}/\hat{\lambda}_0$, the cube root of the ratio of current volume of the membrane to the volume of a sphere of radius $\hat{\lambda}_0 R_0$, which is the current mean radius of the membrane. For Material I, $\hat{\lambda}/\hat{\lambda}_0 = 1.1$ at maximum asphericity. The corresponding deviation of the shape of the deformed membrane from a sphere is difficult to perceive in a line drawing. However, if material points on the membrane are marked as by the manufacturer's seam on a real balloon, the movement of this seam should be the most readily identifiable indicator of asphericity. This seems to be consistent with the observations reported in [1, 2].

Another feature of the equilibrium state at the maximum of ξ_1 consistent with the lack of development of large asphericity is that $t^c\sigma_1$ and $t^c\sigma_2$ are nearly constant and equal throughout the membrane. For example, with Material I and $\bar{\xi}_1 = 0.0001$, at maximum asphericity t^c/t_0 is 0.1 at one pole and 0.43 at the other, compared with $t^c/t_0 = 0.22$ for a sphere homogeneously inflated to the same value of $\hat{\lambda}_0 R_0$, yet the ratio of $t^c\sigma_1$ at the thinner pole to $t^c\sigma_1$ at the thicker pole is 1.03. Of course this means that a significant stress concentration develops at the thinner pole.

As depicted in Fig. 6 considerably less asphericity is developed with Material II. The behavior

in this example is also more sensitive to the magnitude of $\bar{\xi}_1$. The maximum values of ξ_1 are 0.26 and 0.21 for the larger and smaller imperfection amplitudes, respectively, and at maximum asphericity the corresponding values of $u_1^c/\lambda_0 R_0$ are 0.14 and 0.11. In both cases $\hat{\lambda}/\hat{\lambda}_0$ is about 1.01. The maximum asphericity occurs at $\hat{\lambda}_0 = 1.86$ which, as shown in Fig. 4, is when the maximum of σ_0/L_0 occurs.

At least for the two examples considered in Figs. 5 and 6, the behavior of a slightly imperfect spherical membrane correlates well with the curve of σ_0/L_0. Significant growth of the asphericity begins in the vicinity of the bifurcation point, i.e. when $\sigma_0/L_0 = 1/2$, the maximum asphericity occurs when $\hat{\lambda}_0$ is just about equal to the value of λ_0 for which σ_0/L_0 is maximized and the asphericity essentially disappears when σ_0/L_0 falls to 1/2. These two examples suggest that the maximum amplitude of asphericity achieved will increase when the excursion of σ_0/L_0 above 1/2 increases.

As stated previously, for the two examples considered so far the equilibrium paths corresponded to monotonically increasing enclosed volume. A simple example for which this is not the case is illustrated in Fig. 7. Here, a one term strain energy function of the form (11) is considered with $\mu_1 = 8.2$ and $\alpha_1 = 1.2$. Figure 7(a) shows the stress nondimensionalized with respect to $\mu_1\alpha_1$ plotted against stretch for equal biaxial tension. Curves of p^*, the nondimensional pressure (21), and σ_0/L_0 vs stretch are given in Fig. 7(b). After the maximum pressure has been attained, which occurs at $\lambda_0 = 1.36$, the pressure decreases monotonically and no local pressure minimum is achieved. Such behavior is not typical of most rubberlike materials. However, since attention is focussed on the details of the behavior in the vicinity of the bifurcation point, which is $\lambda_0 = 1.61$, nothing need be supposed about the validity of this representation of the material behavior at very large values of λ_0.

Figure 7(c) depicts the curve of bifurcation mode amplitude, ξ_1, vs $\hat{\lambda}_0$ for $\bar{\xi}_1 = 0.001$. The mean radius, $\hat{\lambda}_0$, reaches a maximum and then decreases with increasing asphericity. This contrasts with the previous examples in which $\hat{\lambda}_0$ increased monotonically. The stability of the aspherical equilibrium state is revealed by Fig. 7(d). Initially the enclosed volume $\hat{\lambda}$ is monotonically increasing. However, eventually a local maximum is attained. Note that this occurs after $\hat{\lambda}_0$ has begun to decrease. At the maximum of $\hat{\lambda}$, $\xi_1 = 0.15$. Throughout the range of aspherical deformation depicted in Fig. 7(d) the pressure is decreasing monotonically along the equilibrium path.

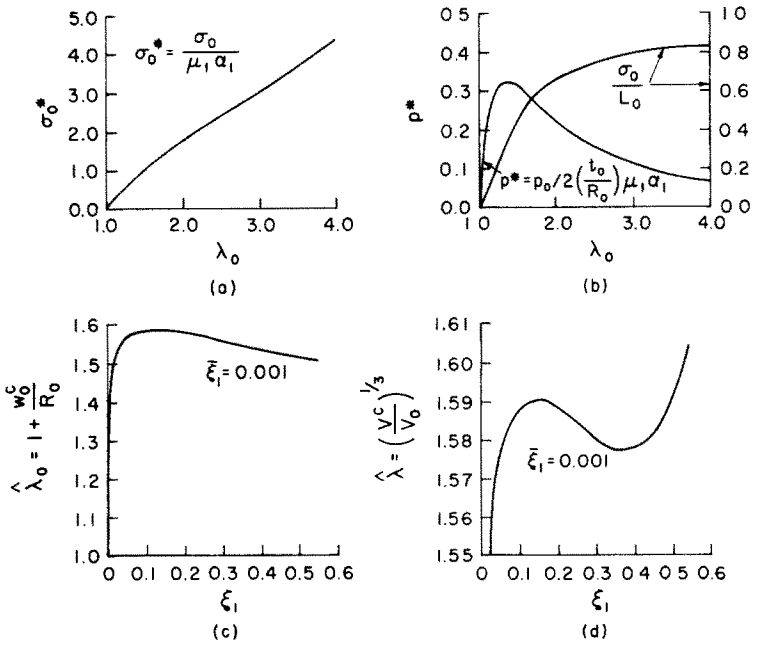

Fig. 7. Behavior of a one term material with $\mu_1 = 8.2$, $\alpha_1 = 1.2$, (a) stress vs stretch curve for equal biaxial tension, (b) curves of pressure and stress divided by instantaneous biaxial stiffness vs stretch, (c) curve of bifurcation mode amplitude vs mean radius and (d) curve of bifurcation mode amplitude vs normalized current volume.

Under prescribed increase in enclosed volume, "snap through" would occur when the maximum of $\hat{\lambda}$ is attained. Then further growth in the aspherical mode would occur stably under the prescribed loading condition, even though $\hat{\lambda}_0$ is decreasing. This example illustrates that if σ_0/L_0 sufficiently exceeds 1/2, an instability can occur even under prescribed change in enclosed volume.

5. CONCLUDING REMARKS

The numerical examples considered have illustrated a number of features associated with the development of aspherical deformation in pressurized elastic spherical membranes. The results indicate that the maximum deviation from sphericity increases with the excursion of σ_0/L_0 above 1/2 and that for a sufficient excursion above 1/2 stability, in the usual engineering sense, with respect to a prescribed increase in enclosed volume is lost. The present results also strongly suggest that the postbifurcation path for a perfect elastic spherical membrane is a closed loop connecting the two bifurcation points, as conjectured by Sewell [2]. This raises the question as to whether or not such a loop always occurs, for physically reasonable elastic constitutive laws, when there are two bifurcation points corresponding to the same mode between the maximum and minimum pressures.

Most aspects of the behavior determined here are in qualitative agreement with the observations in [1, 2] in so far as comparisons can be made. A notable exception is Alexander's [1] observation that the spherically symmetric equilibrium path was rejoined after the pressure minimum. This discrepancy could be due to a number of factors. One possibility is that for the specific rubber and loading condition employed in [1] an instability is encountered on the aspherical equilibrium path and return to the spherical state takes place by "snap through".

Acknowledgements—I am indebted to Dr. M. J. Sewell of Reading University, England, for bringing this phenomenon to my attention and for pointing out a number of useful references. I am also grateful to the Division of Engineering, Brown University, for supporting this work.

REFERENCES

1. H. Alexander, Tensile instability of initially spherical balloons. *Int. J. Engng. Sci.* **9**, 151 (1971).
2. M. J. Sewell, Some mechanical examples of catastrophy theory. *Bull. Inst. Math. Appl.* **12**, 163 (1976).
3. V. I. Feodos'ev, On equilibrium modes of a rubber spherical shell under internal pressure. *PMM* **32**, 339 (1968).
4. A. Needleman, Necking of pressurized spherical membranes. *J. Mech. Phys. Solids* **24** (1976).
5. R. T. Shield, On the stability of finitely deformed elastic membranes—II. *ZAMP* **23**, 16 (1972).
6. R. W. Ogden, Large deformation isotropic elasticity—on the correlation of theory and experiment for incompressible rubberlike solids. *Proc. R. Soc. Lond.* **A. 326**, 565 (1972).
7. B. Budiansky, Notes on nonlinear shell theory. *J. Appl. Mech.* **35**, 393 (1968).
8. L. R. G. Treloar, Stress strain data for vulcanized rubber under various types of deformation. *Trans. Faraday Soc.* **40**, 59 (1944).
9. R. Hill, Some aspects of the incremental behaviour of isotropic elastic solids after finite strain. *Problems in Mechanics: Deformation of Solid Bodies, Novozhilov Anniversary Volume*, p. 459. Leningrad (1969).